Determination of the Adsorption Isotherms of Overpotentially Deposited Hydrogen on a Pt−Ir Alloy in H_2SO_4 Aqueous Solution Using the Phase-Shift Method and Correlation Constants

Jinyoung Chun,[†] Nam Y. Kim,[‡] and Jang H. Chun*[,‡]

Department of Chemical Engineering, Pohang University of Science and Technology, Pohang, Kyungbuk 790-784, Republic of Korea, and Department of Electronic Engineering, Kwangwoon University, Seoul 139-701, Republic of Korea

The phase-shift method and correlation constants, which are unique electrochemical impedance spectroscopy techniques for studying the linear relationship between the phase shift ($90° \geq -\varphi \geq 0°$) versus electric potential (E) behavior for the optimum intermediate frequency and the fractional surface coverage ($0 \leq \theta \leq 1$) vs E behavior, are proposed and verified to determine the Frumkin, Langmuir, and Temkin adsorption isotherms and related electrode kinetic and thermodynamic parameters. On a Pt−Ir [90:10 % (by weight)] alloy in 0.5 M H_2SO_4 aqueous solution, the Frumkin and Temkin adsorption isotherms (θ vs E), equilibrium constants [$K = 3.3 \cdot 10^{-5} \exp(2.5\theta)$ mol^{-1} for the Frumkin and $K = 3.3 \cdot 10^{-4} \exp(-2.1\theta)$ mol^{-1} for the Temkin adsorption isotherm], interaction parameters ($g = -2.5$ for the Frumkin and $g = 2.1$ for the Temkin adsorption isotherm), standard Gibbs energies of adsorption of overpotentially deposited (OPD) H [$(25.6 \geq \Delta G_\theta^0 \geq 19.4)$ kJ·mol^{-1} for $K = 3.3 \cdot 10^{-5} \exp(2.5\theta)$ mol^{-1} and $0 \leq \theta \leq 1$ and $(20.9 < \Delta G_\theta^0 < 24.0)$ kJ·mol^{-1} for $K = 3.3 \cdot 10^{-4} \exp(-2.1\theta)$ mol^{-1} and $0.2 < \theta < 0.8$], and rates of change of ΔG_θ^0 of OPD H with θ ($r = -6.2$ kJ·mol^{-1} for $g = -2.5$ and $r = 5.2$ kJ·mol^{-1} for $g = 2.1$) have been determined and are compared using the phase-shift method and correlation constants. For $0.2 < \theta < 0.8$, a lateral attractive ($g < 0$) or repulsive ($g > 0$) interaction between the adsorbed OPD H species appears. On Pt, Ir, and Pt−Ir alloys in 0.5 M H_2SO_4 aqueous solution, the values of K for the Frumkin adsorption isotherms of OPD H decrease with increasing mass ratio of Ir. Negative values of g for the Frumkin adsorption isotherms of OPD H on the Pt, Ir, and Pt−Ir alloys in acidic and alkaline H_2O and D_2O solutions are experimentally and consistently determined. The duality of the lateral attractive and repulsive interactions is a unique feature of the adsorbed OPD H species on the Pt, Ir, and Pt−Ir alloys in acidic and alkaline H_2O and D_2O solutions.

Introduction

To obtain an environmentally clean energy source, many experimental methods have been used to study the adsorption of H for the cathodic H_2 evolution reaction (HER) on noble metals (alloys) in acidic and alkaline aqueous solutions.[1−7] It is well-known that underpotentially deposited hydrogen (UPD H) and overpotentially deposited hydrogen (OPD H) occupy different surface adsorption sites and act as two distinguishable electroadsorbed H species and that only OPD H can contribute to the cathodic HER.[2,4,5,7]

Although the Frumkin and Langmuir adsorption isotherms may be regarded as classical models and theories, it is preferable to consider the Frumkin and Langmuir adsorption isotherms for OPD H rather than equations of the electrode kinetics and thermodynamics for OPD H because these adsorption isotherms are associated more directly with the atomic mechanism of OPD H.[8] However, there is not much reliable information on the Frumkin and Langmuir adsorption isotherms of OPD H and related electrode kinetic and thermodynamic data. Furthermore, a negative value of the interaction parameter for the Frumkin adsorption isotherm of OPD H has not been frequently discussed on the basis of relevant experimental data.[2,4,5,7] Thus, there is a technological need for a simple, accurate, and reliable method to determine the Frumkin, Langmuir, and Temkin adsorption isotherms for characterizing the adsorption of intermediates (OPD H) for sequential reactions (HER) on noble metals (alloys) in acidic and alkaline aqueous solutions.

Many scientific phenomena have been interpreted by their behavior rather than by their nature. For example, the wave-particle duality of light and electrons (i.e., their wave and particle behaviors) is well-known in science and has been applied in engineering. Notably, these wave and particle behaviors are complementary rather than contradictory to each other. The phase-shift method and correlation constants are unique electrochemical impedance spectroscopy techniques for studying the linear relationship between the phase shift ($90° \geq -\varphi \geq 0°$) versus electric potential (E) behavior for the optimum intermediate frequency and the fractional surface coverage ($0 \leq \theta \leq 1$) vs E behavior of intermediates for sequential reactions on noble and highly corrosion-resistant metals (alloys) in acidic and alkaline H_2O and D_2O solutions.[9−28] The θ versus E behavior of the fractional surface coverage is well-known as the Frumkin or Langmuir adsorption isotherm.

New ideas or methods must be rigorously tested, especially when they are unique, but only with pure logic and objectivity and through scientific procedures. However, the objections to the phase-shift method[29−31] do not fulfill these criteria. These objections are substantially attributed to confusion and misunderstanding about the phase-shift method itself.[26−28,32,33] It

* Author to whom correspondence should be addressed. E-mail: jhchun@kw.ac.kr. Fax: +82-2-942-5235. Tel: +82-2-940-5116.
[†] Pohang University of Science and Technology.
[‡] Kwangwoon University.

10.1021/je100837q
Published on Web 01/05/2011

should especially be noted that all of the objections to the phase-shift method[29,31] can be attributed to confusion and misunderstanding about the applicability of related equations for intermediate frequencies and a unique feature of the Faradaic resistances for the recombination steps.[26−28,34]

In practice, the numerical calculation or simulation of equivalent circuit impedances of metals (alloys) in solutions is very difficult or impossible due to the superposition of various effects. However, it is simply determined or measured by frequency analyzers, that is, instruments or tools. It should be noted that the phase-shift method and correlation constants are a useful and efficient tool for determining the Frumkin, Langmuir, and Temkin adsorption isotherms. The validity and correctness of the phase-shift method should be discussed on the basis of simulations with a single equation for $-\varphi$ versus θ as functions of E and frequency (f) or relevant experimental results which are obtained using other conventional methods. However, the single equation for $-\varphi$ versus θ as functions of E and f has never been derived or discussed on the basis of relevant experimental results.[29−31] The simulations of the phase-shift method without this single equation, that is, $-\varphi$ versus θ, are basically meaningless or in vain.[26−28,32−34] It should be noted that this problem has been experimentally and consistently solved using the phase-shift method for determining adsorption isotherms.

In this paper, we present and compare the Frumkin and Temkin adsorption isotherms of OPD H and related electrode kinetic and thermodynamic parameters of a Pt−Ir [90:10 % (by weight)] alloy in 0.5 M H_2SO_4 aqueous solution using the phase-shift method and correlation constants. A negative value of the interaction parameter for the Frumkin adsorption isotherms of OPD H on Pt, Ir, and Pt−Ir alloys in 0.5 M H_2SO_4 and 0.1 M KOH aqueous solutions has also been discussed. On the Pt, Ir, and Pt−Ir alloys in 0.5 M H_2SO_4 aqueous solution, the mass ratio effect on the Frumkin and Temkin adsorption isotherms of OPD H is summarized. This paper is a supplement to previously published papers.[21,22]

Experimental Section

Preparations. With the H^+ concentration and the effects of the diffuse double layer and pH taken into account,[35] 0.5 M H_2SO_4 aqueous solution (pH 0.46) was prepared from H_2SO_4 (Sigma-Aldrich, reagent grade) using purified water (H_2O, resistivity >18 MΩ·cm) obtained from a Millipore system. The 0.5 M H_2SO_4 aqueous solution was deaerated with 99.999 % purified nitrogen gas for 20 min before the experiments. A standard three-electrode configuration was employed. A saturated calomel electrode (SCE) was used as the standard reference electrode. A platinum−iridium alloy wire [Johnson Matthey, Pt/Ir; 90:10 % (by weight), 1.5 mm diameter, estimated surface area ca. 0.94 cm^2] and a platinum wire (Johnson Matthey, purity 99.95 %, 1.5 mm diameter, estimated surface area ca. 1.94 cm^2) were used as the working electrode and the counter electrode, respectively. Both the Pt−Ir alloy working electrode and the Pt counter electrode were prepared by flame cleaning and then quenched and cooled sequentially in Millipore Milli-Q water and air.

Measurements. A cyclic voltammetry (CV) technique was used to achieve a steady state on the Pt−Ir alloy in 0.5 M H_2SO_4 aqueous solution. The CV experiments were conducted for 25 cycles at a scan rate of 200 mV·s^{-1} and a scan potential of (−0.241 to 1.0) V versus SCE. After the CV experiments, an electrochemical impedance spectroscopy (EIS) technique was used to study the linear relationship between the $-\varphi$ versus E behavior of the phase shift ($90° \geq -\varphi \geq 0°$) for the optimum intermediate frequency and the θ versus E behavior of the fractional surface coverage ($0 \leq \theta \leq 1$) on the Pt−Ir alloy in 0.5 M H_2SO_4 aqueous solution. The EIS experiments were conducted at scan frequencies of (10^4 to 1) Hz, a single sine wave, an alternating current (ac) amplitude of 5 mV, and a direct current (dc) potential of (0 to −0.450) V versus SCE.

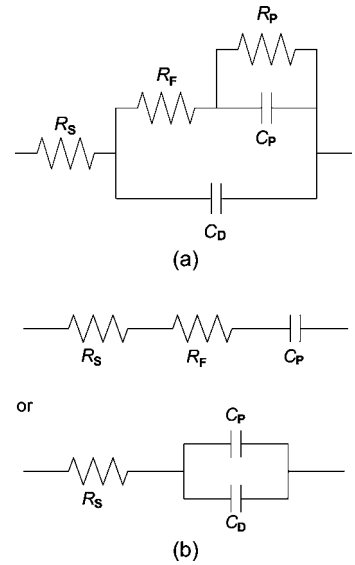

Figure 1. (a) Experimentally proposed equivalent circuit for the phase-shift method and (b) simplified equivalent circuit for intermediate frequency responses.

The CV experiments were performed using an EG&G PAR model 273A potentiostat controlled with the PAR model 270 software package. The EIS experiments were performed using the same apparatus in conjunction with a Schlumberger SI 1255 HF Frequency Response analyzer controlled with the PAR model 398 software package. To obtain comparable and reproducible results, all of the measurements were carried out using the same preparations, procedures, and conditions at 298 K. The international sign convention is used: cathodic currents and phase shifts or angles are taken as negative. All potentials are given on the standard hydrogen electrode (SHE) scale. The Gaussian and adsorption isotherm analyses were carried out using the Excel and Origin software packages.

Results and Discussion

Theoretical and Experimental Backgrounds of the Phase-Shift Method. The equivalent circuit for the adsorption of OPD H for the cathodic HER on the Pt−Ir alloy in 0.5 M H_2SO_4 aqueous solution can be expressed as shown in Figure 1a.[26−28,36−38] Taking into account the superposition of various effects (relaxation time effects, real surface area problems, surface absorption and diffusion processes, inhomogeneous and lateral interaction effects, oxide layer formations, specific adsorption effects, etc.) that are inevitable under the experimental conditions, we define the equivalent circuit elements as follows: R_S is the real solution resistance; R_F is the real resistance due to the Faradaic resistance (R_ϕ) for the discharge step and superposition of various effects; R_P is the real resistance due to the Faradaic resistance (R_R) for the recombination step and superposition of various effects; C_P is the real capacitance due to the adsorption pseudocapacitance (C_ϕ) and superposition of various effects; and C_D is the real double-layer capacitance. Correspondingly, neither R_F nor C_P is constant; both depend

Table 1. Measured Values of the Phase Shift ($-\varphi$) for the Optimum Intermediate Frequency (f_o = 25.12 Hz), the Estimated Fractional Surface Coverage (θ) of OPD H, and the Normalized Change Rates [$\Delta(-\varphi)/\Delta E$, $\Delta\theta/\Delta E$] on the Pt−Ir Alloy in 0.5 M H_2SO_4 Aqueous Solution

E	$-\varphi$		$\Delta(-\varphi)$	$\Delta\theta$
V vs SHE	deg	θ ($0 \le \theta \le 1$)	ΔE	ΔE
0.061	82.4	≈ 0	≈ 0	≈ 0
0.041	82.2	0.00245	0.02451	0.02451
0.021	78.6	0.04657	0.44118	0.44118
0.001	64.6	0.21814	1.71569	1.71569
−0.019	40.0	0.51961	3.01471	3.01471
−0.039	19.3	0.77328	2.53676	2.53676
−0.059	6.9	0.92525	1.51961	1.51961
−0.079	2.8	0.97549	0.50245	0.50245
−0.099	1.3	0.99387	0.18382	0.18382
−0.119	0.9	0.99877	0.04902	0.04902
−0.139	0.8	≈ 1	0.01225	0.01225

on E and θ and can be measured. It should be noted that both R_ϕ and C_ϕ also depend on E and θ but cannot be measured.

The numerical derivation of C_ϕ from the Frumkin and Langmuir adsorption isotherms (θ vs E) is described elsewhere, and R_ϕ depends on C_ϕ.[36,37] A unique feature of R_ϕ and C_ϕ is that they attain maximum values at $\theta \approx 0.5$ and intermediate E, decrease symmetrically with E at other values of θ, and approach minimum values at $\theta \approx 0$ and low E and $\theta \approx 1$ and high E; this behavior is well-known in interfacial electrochemistry, electrode kinetics, and EIS. The unique feature and combination of R_ϕ and C_ϕ versus E imply that the normalized rate of change of $-\varphi$ with respect to E, that is, $\Delta(-\varphi)/\Delta E$, corresponds to that of θ versus E, that is, $\Delta\theta/\Delta E$, and vice versa. Both $\Delta(-\varphi)/\Delta E$ and $\Delta\theta/\Delta E$ are maximized at $\theta \approx 0.5$ and intermediate E, decrease symmetrically with E at other values of θ, and are minimized at $\theta \approx 0$ and low E and $\theta \approx 1$ and high E. Correspondingly, the values of $\Delta(-\varphi)/\Delta E$ and $\Delta\theta/\Delta E$ at the optimum intermediate frequency (f_o) are exactly the same (see Table 1). The linear relationship between and Gaussian profiles of $-\varphi$ versus E or $\Delta(-\varphi)/\Delta E$ and θ versus E or $\Delta\theta/\Delta E$ most clearly appear at f_o. The value of f_o is experimentally and graphically evaluated on the basis of $\Delta(-\varphi)/\Delta E$ and $\Delta\theta/\Delta E$ for intermediate and other frequencies (see Figures 3 to 5). The importance of f_o is described elsewhere.[22] The linear relationship between and Gaussian profiles of $-\varphi$ versus E or $\Delta(-\varphi)/\Delta E$ and θ versus E or $\Delta\theta/\Delta E$ at f_o imply that only one Frumkin or Langmuir adsorption isotherm is determined on the basis of the relevant experimental results (see Table 1 and Figures 3 to 5). Notably, this is not a mere coincidence but a unique feature of the Frumkin and Langmuir adsorption isotherms (θ vs E). These aspects are the essential nature of the phase-shift method and correlation constants for determining the Frumkin and Langmuir adsorption isotherms.

The frequency responses of the equivalent circuit for all f shown in Figure 1a are essential for understanding the unique feature and combination of R_ϕ and C_ϕ versus E, that is, the linear relationship between and Gaussian profiles of $-\varphi$ versus E or $\Delta(-\varphi)/\Delta E$ and θ versus E or $\Delta\theta/\Delta E$ at f_o. At very low frequencies, the equivalent circuit for all f can be expressed as a series circuit of R_S, R_F, and R_P. At very high frequencies, the equivalent circuit for all f can be expressed as a series circuit of R_S and C_D. At intermediate frequencies, one finds regions in which the equivalent circuit for all f behaves as a series circuit of R_S, R_F, and C_P or a series and parallel circuit of R_S, C_P, and C_D, as shown in Figure 1b.[26−28,36,37] However, it should be noted that the simplified equivalent circuit shown in Figure 1b does not represent the change of the cathodic HER itself but only the intermediate frequency response.

At intermediate frequencies, the impedance (Z) and phase shift ($-\varphi$) are given by[26−28]

$$Z = R_S + R_F - \frac{j}{\omega C_P} \tag{1a}$$

$$-\varphi = \arctan\left[\frac{1}{\omega(R_S + R_F)C_P}\right] \tag{1b}$$

for the upper circuit in Figure 1b or

$$Z = R_S - \frac{j}{\omega(C_P + C_D)} \tag{2a}$$

$$-\varphi = \arctan\left[\frac{1}{\omega R_S(C_P + C_D)}\right] \tag{2b}$$

for the lower circuit in Figure 1b, where j is the imaginary unit (i.e., $j^2 = -1$) and ω is the angular frequency, defined as $\omega = 2\pi f$, where f is the frequency. Under these conditions,

$$R_P \gg \frac{1}{\omega C_P} \text{ and } R_P \gg R_S + R_F \tag{3}$$

In our previously published papers,[9−25] only eq 1a was used with a footnote stating that C_P practically includes C_D (see Tables 1 and 2 in ref 21, Table 1 in ref 20, etc.). Both eqs 1a and 2a show that the effect of R_P on $-\varphi$ for intermediate frequencies is negligible. These aspects are completely overlooked, confused, and misunderstood in the comments on the phase-shift method by Horvat-Radosevic, Kvastek, and Lasia.[29−31] Correspondingly, all of the simulations of the phase-shift method using eq 1a that appear in these comments (where C_P does not include C_D)[29−31] are basically invalid or wrong. All of the analyses of the effect of R_P on $-\varphi$ for intermediate frequencies are also invalid or wrong (see Supporting Information).[26−28,34]

The following limitations and conditions of the equivalent circuit elements for f_o are summarized on the basis of the experimental data.[9−28] Neither R_S nor C_D is constant. At $\theta \approx 0$, $R_S > R_F$ and $C_D > C_P$, or vice versa, and so forth. For a wide range of θ ($0.2 < \theta < 0.8$), $R_F \gg R_S$ or $R_F > R_S$ and $C_P \gg C_D$ or $C_P > C_D$, and so forth. At $\theta \approx 1$, $R_S > R_F$ or $R_S < R_F$ and $C_P \gg C_D$. The measured $-\varphi$ for f_o depends on E and θ. In contrast to numerical calculations or analyses, these limitations and conditions for eq 1a or 2a are not considered for the phase-shift method because all of the measured values of $-\varphi$ for intermediate frequencies include (R_S, R_F) and (C_P, C_D). Correspondingly, the measured $-\varphi$ for f_o is valid and correct regardless of the applicability of eq 1a or 2a and related limitations and conditions (see Supplementary Table 1, Supporting Information). This is the reason why the phase-shift method is the most useful and effective way to determine adsorption isotherms.

The unique feature and combination of (R_S, R_F) and (C_P, C_D) are equivalent to those of R_ϕ and C_ϕ. This is attributed to the reciprocal property of R_F and C_P and suggests that only the polar form of the equivalent circuit impedance, that is, $-\varphi$ described in eq 1b or 2b, is useful and effective for studying the linear relationship between the $-\varphi$ versus E behavior ($90° \ge -\varphi \ge 0°$) at f_o and the θ versus E behavior ($0 \le \theta \le 1$). It should be noted that the phase-shift method for determining adsorption

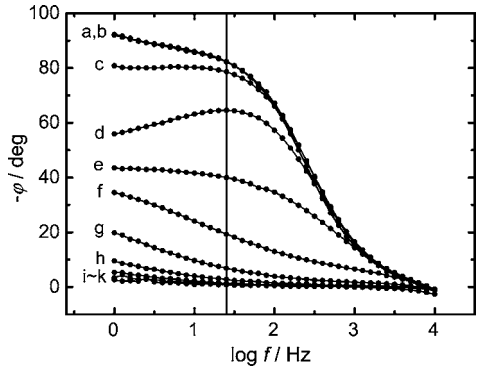

Figure 2. Comparison of the phase-shift curves ($-\varphi$ vs log f) on the Pt−Ir alloy in 0.5 M H_2SO_4 aqueous solution. Vertical solid line: 25.12 Hz; single sine wave; scan frequency: (10^4 to 1) Hz; ac amplitude: 5 mV; dc potential: (a) 0.061 V, (b) 0.041 V, (c) 0.021 V, (d) 0.001 V, (e) −0.019 V, (f) −0.039 V, (g) −0.059 V, (h) −0.079 V, (i) −0.099 V, (j) −0.119 V, and (k) −0.139 V versus SHE.

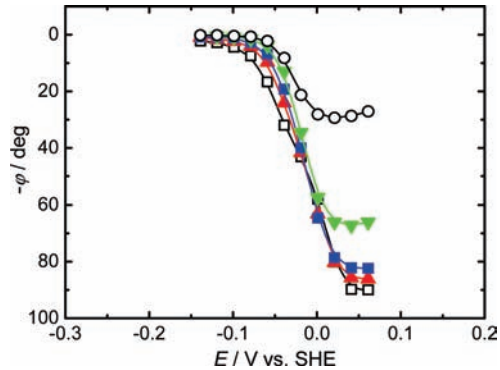

Figure 3. Comparison of the phase-shift profiles ($-\varphi$ vs E) for five different frequencies on the Pt−Ir alloy in 0.5 M H_2SO_4 aqueous solution. Measured values: □, 1.995 Hz; red triangles, 10 Hz; blue squares, 25.12 Hz; green triangles, 100 Hz; ○, 501.2 Hz. The optimum intermediate frequency is 25.12 Hz (blue square).

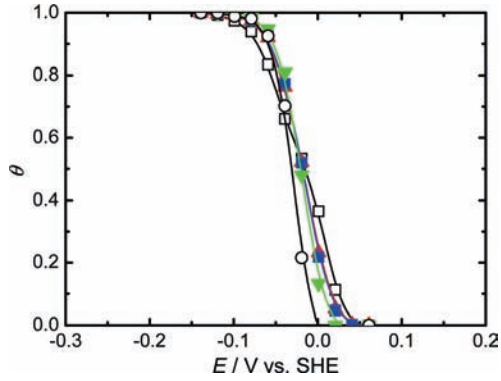

Figure 4. Comparison of the surface-coverage profiles (θ vs E) for five different frequencies on the Pt−Ir alloy in 0.5 M H_2SO_4 aqueous solution. Estimated values: □, 1.995 Hz; red triangles, 10 Hz; blue squares, 25.12 Hz; green triangles, 100 Hz; ○, 501.2 Hz. The optimum intermediate frequency is 25.12 Hz (blue square).

isotherms has been proposed and verified on the basis of the phase-shift curves ($-\varphi$ vs log f) at various E (see Figure 2). These aspects have been experimentally and consistently verified and discussed in our previously published papers.[9−28] As stated above, the unique feature and combination of R_ϕ and C_ϕ versus E, that is, $\Delta(-\varphi)/\Delta E$ and $\Delta\theta/\Delta E$, most clearly appear at f_o. The linear relationship between and Gaussian profiles of $-\varphi$ versus E or $\Delta(-\varphi)/\Delta E$ and θ versus E or $\Delta\theta/\Delta E$ for f_o imply that only one Frumkin or Langmuir adsorption isotherm is determined on the basis of the relevant experimental results (see Figures 2 to 6). The shape and location of the $-\varphi$ versus E or $\Delta(-\varphi)/\Delta E$ curve and θ versus E or $\Delta\theta/\Delta E$ curve for f_o correspond to the interaction parameter (g) and equilibrium constant (K_o) for the Frumkin or Langmuir adsorption isotherm, respectively. This is another reason why the phase-shift method is the most accurate way to determine adsorption isotherms.

Basic Procedure and Description of the Phase-Shift Method. Figure 2 compares the phase-shift curves ($-\varphi$ vs log f) for different potentials (E) on the Pt−Ir alloy in 0.5 M H_2SO_4 aqueous solution. The intermediate frequency of 25.12 Hz, shown as a vertical solid line on the $-\varphi$ versus log f plot in Figure 2, can be set as f_o for $-\varphi$ versus E and θ versus E. At the maximum $-\varphi$ shown in curve a of Figure 2, it appears that the adsorption of OPD H and superposition of various effects are minimized; that is, $\theta \approx 0$ and E is low. It should be noted that θ ($0 \le \theta \le 1$) depends on E. At the maximum $-\varphi$, when $\theta \approx 0$ and E is low, both $\Delta(-\varphi)/\Delta E$ and $\Delta\theta/\Delta E$ are minimized because R_ϕ and C_ϕ approach minimum values. At the minimum $-\varphi$ shown in curve k of Figure 2, it appears that the adsorption of OPD H and superposition of various effects are maximized or almost saturated; that is, $\theta \approx 1$ and E is high. At the minimum $-\varphi$, when $\theta \approx 1$ and E is high, both $\Delta(-\varphi)/\Delta E$ and $\Delta\theta/\Delta E$ are also minimized because R_ϕ and C_ϕ approach minimum values. At the medium $-\varphi$ between curves d and e of Figure 2, it appears that both $\Delta(-\varphi)/\Delta E$ and $\Delta\theta/\Delta E$ are maximized because R_ϕ and C_ϕ approach maximum values at $\theta \approx 0.5$ and intermediate E (see Figure 5c).

The procedure and description of the phase-shift method for determining the Frumkin adsorption isotherm of OPD H on the Pt−Ir alloy in 0.5 M H_2SO_4 aqueous solution are briefly summarized in Table 1. Table 1 shows the values of $-\varphi$ and θ as functions of E at $f_o = 25.12$ Hz with −20 mV increment changes in E on the Pt−Ir alloy in 0.5 M H_2SO_4 aqueous solution. The values of $-\varphi$ and θ as functions of E at $f_o = 25.12$ Hz shown in Figures 3 and 4 are illustrated on the basis of the experimental results summarized in Table 1. The values of $-\varphi$ and θ as functions of E at other frequencies (1.995 Hz, 10 Hz, 100 Hz, and 501.2 Hz) shown in Figures 3 and 4 are also illustrated through the same procedures summarized in Table 1.

As shown in Figures 2 to 4, $-\varphi$ depends on both f and E. However, θ depends on only E. As previously described, the linear relationship between and Gaussian profiles of $-\varphi$ versus E or $\Delta(-\varphi)/\Delta E$ and θ versus E or $\Delta\theta/\Delta E$ most clearly appear at f_o. This is the reason why the comparison of $-\varphi$ versus E and θ versus E for different frequencies shown in Figures 3 and 4 is necessary to determine f_o. It should be noted that the $-\varphi$ versus E profiles shown in Figure 3 correspond to the θ versus E profiles shown in Figure 4 and vice versa. The differences between the $-\varphi$ versus E and θ versus E profiles at $f_o = 25.12$ Hz and those at other frequencies (1.995 Hz, 10 Hz, 100 Hz, and 501.2 Hz) shown in Figures 3 and 4 do not represent the measurement error but only the frequency response.

Figure 5 compares the normalized rates of change of $-\varphi$ and θ with respect to E, that is, $\Delta(-\varphi)/\Delta E$ and $\Delta\theta/\Delta E$, for five different frequencies (1.995 Hz, 10 Hz, 25.12 Hz, 100 Hz, and 501.2 Hz) on the Pt−Ir alloy in 0.5 M H_2SO_4 aqueous solution. The Gaussian profile shown in Figure 5c is based on the $\Delta(-\varphi)/\Delta E$ and $\Delta\theta/\Delta E$ data for $f_o = 25.12$ Hz summarized in Table 1. Similarly, the Gaussian profiles for other frequencies (1.995 Hz, 10 Hz, 100 Hz, and 501.2 Hz) shown in Figure 5 were obtained through the same procedures summarized in Table 1. In Figure 5c, $\Delta(-\varphi)/\Delta E$ corresponds to $\Delta\theta/\Delta E$ and vice versa. Both $\Delta(-\varphi)/\Delta E$ and $\Delta\theta/\Delta E$ are maximized at the medium $-\varphi$ when

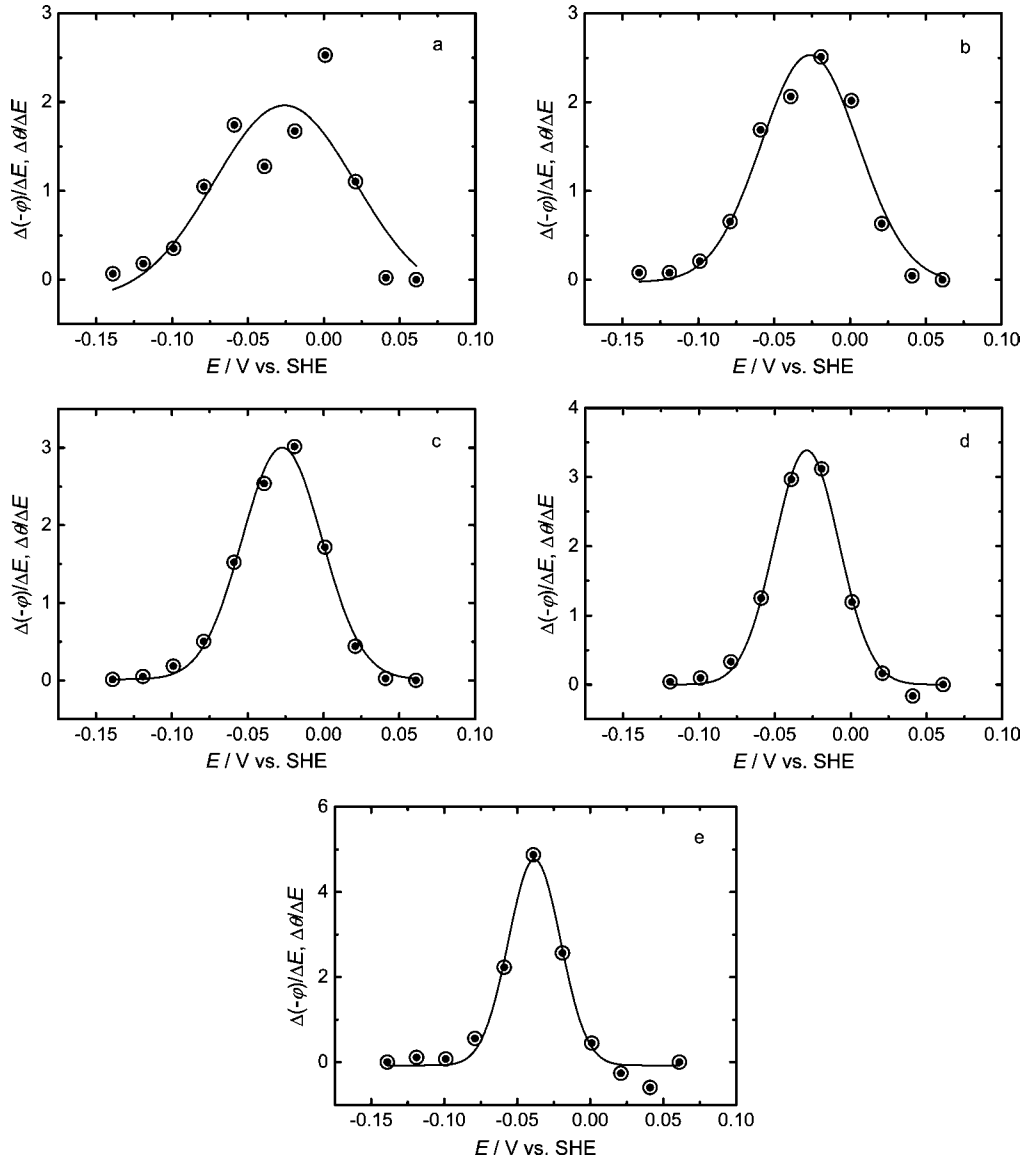

Figure 5. Comparison of the normalized rates of change of $-\varphi$ and θ with respect to E, that is, $\Delta(-\varphi)/\Delta E$ and $\Delta\theta/\Delta E$, for five different frequencies on the Pt−Ir alloy in 0.5 M H_2SO_4 aqueous solution. —, Fitted Gaussian profile; ○, $\Delta(-\varphi)/\Delta E$; ●, $\Delta\theta/\Delta E$. (a) 1.995 Hz, (b) 10 Hz, (c) 25.12 Hz, (d) 100 Hz, and (e) 501.2 Hz. The optimum intermediate frequency is 25.12 Hz.

$\theta \approx 0.5$ and E is intermediate, decrease symmetrically with E at other values of θ, and are minimized at the maximum $-\varphi$ when $\theta \approx 0$ and E is low and the minimum $-\varphi$ when $\theta \approx 1$ and E is high. As previously described, this is a unique feature of the Frumkin and Langmuir adsorption isotherms. The shape and location of the $-\varphi$ versus E or $\Delta(-\varphi)/\Delta E$ curve and the θ versus E or $\Delta\theta/\Delta E$ curve at f_o correspond to the interaction parameter (g) and equilibrium constant (K_o) for the Frumkin or Langmuir adsorption isotherm, respectively. The differences between the Gaussian profiles of $\Delta(-\varphi)/\Delta E$ and $\Delta\theta/\Delta E$ at f_o = 25.12 Hz and those at other frequencies (1.995 Hz, 10 Hz, 100 Hz, and 501.2 Hz) shown in Figure 5 do not represent the measurement error but only the frequency response.

Finally, one can conclude that the Frumkin or Langmuir adsorption isotherm corresponding to $\Delta(-\varphi)/\Delta E$ and $\Delta\theta/\Delta E$ at f_o is readily determined. The linear relationship between and Gaussian profiles of the $-\varphi$ versus E or $\Delta(-\varphi)/\Delta E$ curve and the θ versus E or $\Delta\theta/\Delta E$ curve at f_o express the essential nature of the phase-shift method and correlation constants for determining the Frumkin or Langmuir adsorption isotherm. Notably, this is not valid and correct at all f and E but only at f_o for a limited range of E.

The Frumkin, Langmuir, and Temkin Adsorption Isotherms. The derivation and interpretation of the practical forms of the electrochemical Frumkin, Langmuir, and Temkin adsorption isotherms are described elsewhere.[39−42] The Frumkin adsorption isotherm assumes that the Pt−Ir alloy surface is inhomogeneous or that the lateral interaction effect is not negligible. The Frumkin adsorption isotherm can be expressed as follows:[40]

$$\left[\frac{\theta}{1-\theta}\right]\exp(g\theta) = K_o C^+ \exp(-EF/RT) \tag{4}$$

$$g = \frac{r}{RT} \tag{5}$$

$$K = K_o \exp(-g\theta) \tag{6}$$

where θ ($0 \le \theta \le 1$) is the fractional surface coverage, g is the interaction parameter for the Frumkin adsorption isotherm, K_o

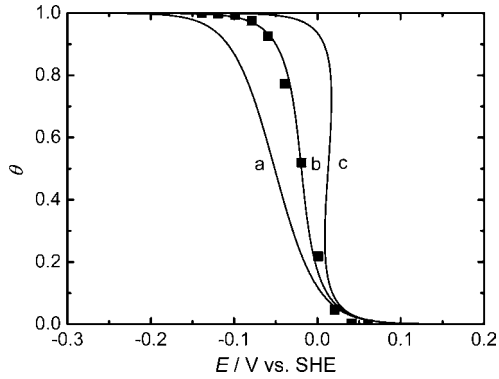

Figure 6. Comparison of the experimental and fitted data for the Frumkin adsorption isotherms (θ vs E) of OPD H on the Pt−Ir alloy in 0.5 M H_2SO_4 aqueous solution. Experimental data: ■. Calculated value using eq 4 (Frumkin adsorption isotherm): —. (a) $g = 0$, that is, the Langmuir adsorption isotherm, (b) $g = -2.5$, and (c) $g = -5$ for $K_o = 3.3 \cdot 10^{-5}$ mol^{-1}. The Frumkin adsorption isotherm shown in curve b of Figure 6 is $K = 3.3 \cdot 10^{-5} \exp(2.5\theta)$ mol^{-1}.

is the equilibrium constant at $g = 0$, C^+ is the concentration of ions (H^+) in the bulk solution, E is the negative potential, F is Faraday's constant, R is the gas constant, T is the absolute temperature, r is the rate of change of the standard Gibbs energy of adsorption with θ, and K is the equilibrium constant. The dimension of K is described elsewhere.[43] It should be noted that when $g = 0$ in eqs 4 to 6, the Langmuir adsorption isotherm is obtained. For the Langmuir adsorption isotherm, when $g = 0$, the inhomogeneous and lateral interaction effects on the adsorption are assumed to be negligible.

On the Pt−Ir alloy in 0.5 M H_2SO_4 aqueous solution, the numerically calculated Frumkin adsorption isotherms using eq 4 are shown in Figure 6. Curves a, b, and c in Figure 6 show the three numerically calculated Frumkin adsorption isotherms corresponding to $g = 0$, -2.5, and -5, respectively, for $K_o = 3.3 \cdot 10^{-5}$ mol^{-1}. Curve a, with $g = 0$ for $K_o = 3.3 \cdot 10^{-5}$ mol^{-1}, corresponds to the Langmuir adsorption isotherm, that is, $K = 3.3 \cdot 10^{-5}$ mol^{-1}. Curve b in Figure 6 shows that the Frumkin adsorption isotherm $K = 3.3 \cdot 10^{-5} \exp(2.5\theta)$ mol^{-1} is applicable to the adsorption of OPD H, and eq 5 gives $r = -6.2$ kJ·mol^{-1}.

The comparison of the experimental and fitted data for the Frumkin adsorption isotherms of OPD H on Pt, Ir, and Pt−Ir alloys in 0.5 M H_2SO_4 and 0.1 M KOH aqueous solutions is shown in Supplementary Figures 1 and 2, respectively (Supporting Information).[21,22,26] On the Pt, Ir, and Pt−Ir alloys in 0.5 M H_2SO_4 aqueous solution, the values of K for the Frumkin adsorption isotherms of OPD H decrease with increasing mass ratio of Ir (see Table 2 and Supplementary Figure 1, Supporting Information).

At intermediate values of θ (i.e., $0.2 < \theta < 0.8$), the pre-exponential term, $\theta/(1 - \theta)$, varies little with θ in comparison with the variation of the exponential term, $\exp(g\theta)$ (see eq 4). Under these approximate conditions, the Temkin adsorption isotherm can be simply derived from the Frumkin adsorption isotherm. The Temkin adsorption isotherm can be expressed as follows:[40]

$$\exp(g\theta) = K_o C^+ \exp(-EF/RT) \qquad (7)$$

Figure 7 shows the determination of the Temkin adsorption isotherm corresponding to the Frumkin adsorption isotherm shown in curve b of Figure 6. Dashed line b in Figure 7 shows

Table 2. Comparison of the Standard Gibbs Energies of Adsorption (ΔG_θ^0) of OPD H and the Equilibrium Constants (K) for the Frumkin Adsorption Isotherms (θ vs E) of OPD H on the Pt, Ir, and Pt−Ir Alloys in 0.5 M H_2SO_4 and 0.1 M KOH Aqueous Solutions

	ΔG_θ^0	K	
metal (alloy)/solution	kJ·mol^{-1}	mol^{-1}	ref
Pt−Ir alloy[a]/0.5 M H_2SO_4	$25.6 \geq \Delta G_\theta^0 \geq 19.4$	$3.3 \cdot 10^{-5} \exp(2.5\theta)$	this work
Pt−Ir alloy[b]/0.5 M H_2SO_4	$25.7 \geq \Delta G_\theta^0 \geq 19.5$	$3.1 \cdot 10^{-5} \exp(2.5\theta)$	21
Pt[c]/0.5 M H_2SO_4	$25.4 \geq \Delta G_\theta^0 \geq 19.5$	$3.5 \cdot 10^{-5} \exp(2.4\theta)$	22
Ir[d]/0.5 M H_2SO_4	$26.1 \geq \Delta G_\theta^0 \geq 20.1$	$2.7 \cdot 10^{-5} \exp(2.4\theta)$	22
Pt[e]/0.1 M KOH	$22.4 \geq \Delta G_\theta^0 \geq 16.5$	$1.2 \cdot 10^{-4} \exp(2.4\theta)$	26
Ir[f]/0.1 M KOH	$23.0 \geq \Delta G_\theta^0 \geq 17.1$	$9.4 \cdot 10^{-5} \exp(2.4\theta)$	26

[a] Pt−Ir [90:10 % (by weight)] alloy. [b] Pt−Ir [70:30 % (by weight)] alloy. [c] Pt (purity: 99.9985 %). [d] Ir (purity: 99.8 %). [e] Pt (purity: 99.9985 %). [f] Ir (purity: 99.8 %). The Frumkin adsorption isotherms (θ vs E) are valid and effective for $0 \leq \theta \leq 1$.

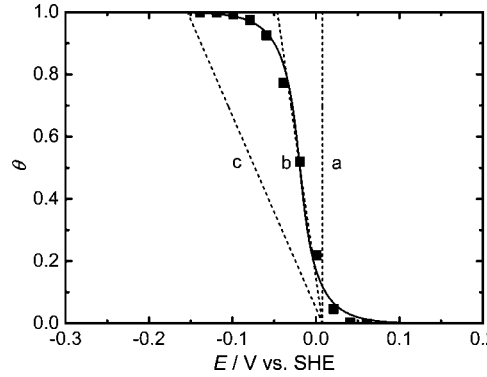

Figure 7. Comparison of the experimentally determined Frumkin and three fitted Temkin adsorption isotherms (θ vs E) of OPD H on the Pt−Ir alloy in 0.5 M H_2SO_4 aqueous solution. Experimental data: ■. Calculated value using eq 4 (Frumkin adsorption isotherm): —. Calculated value using eq 7 (Temkin adsorption isotherm) and the correlation constants: ----. (a) $g = 0$, (b) $g = 2.1$, and (c) $g = 6.3$ for $K_o = 3.3 \cdot 10^{-4}$ mol^{-1}. The Temkin adsorption isotherm shown in dashed line b of Figure 7, $K = 3.3 \cdot 10^{-4} \exp(-2.1\theta)$ mol^{-1}, is valid and effective only for $0.2 < \theta < 0.8$.

that the numerically calculated Temkin adsorption isotherm using eq 7 is $K = 3.3 \cdot 10^{-4} \exp(-2.1\theta)$ mol^{-1}, and eq 5 gives $r = 5.2$ kJ·mol^{-1}. The applicability of the Frumkin and Temkin adsorption isotherms over the same potential range is described elsewhere.[26] As shown in dashed line b of Figure 7, the Temkin adsorption isotherm is valid and effective only for $0.2 < \theta < 0.8$. This θ range corresponds to a short potential range (ca. 33 mV).

Correlation Constants between the Adsorption Isotherms. As previously described, the Frumkin, Langmuir, and Temkin adsorption conditions are different from each other. Only one Frumkin or Langmuir adsorption isotherm is determined on the basis of the relevant experimental results (see Figures 2 to 6). However, the two different adsorption isotherms, that is, the Temkin and Frumkin or Langmuir adsorption isotherms, appear to fit the same data for $0.2 < \theta < 0.8$. This unique feature of the Temkin and Frumkin or Langmuir adsorption isotherms has been experimentally and consistently verified using the phase-shift method and correlation constants.[20−28] For $0.2 < \theta < 0.8$, the Temkin adsorption isotherm correlating with the Frumkin or Langmuir adsorption isotherm, and vice versa, is readily determined using the correlation constants.

In this work, one can also confirm that the values of g and K_o for the Temkin adsorption isotherm are approximately 4.6 and 10 times greater than those for the correlated Frumkin or

Langmuir adsorption isotherm, respectively. These factors (ca. 4.6 and 10) can be taken as correlation constants between the Temkin and Frumkin or Langmuir adsorption isotherms. The two different adsorption isotherms, that is, the Temkin and Frumkin or Langmuir adsorption isotherms, appear to fit the same data regardless of their adsorption conditions. This aspect is described elsewhere.[20,21,24−28]

Negative Value of the Interaction Parameter. A negative value of the interaction parameter (g) for the Frumkin adsorption isotherm is qualitatively and quantitatively interpreted elsewhere.[40,44] The negative value of g for the Frumkin adsorption isotherm shown in curve b of Figure 6 implies a lateral attractive interaction between the adsorbed OPD H species, which leads to an increase in the absolute value of the standard Gibbs energy ($|\Delta G_\theta^0|$) of OPD H with θ ($0 \le \theta \le 1$).[40] This interaction is a unique feature of the Frumkin adsorption isotherms of OPD H on the Pt, Ir, and Pt−Ir alloys in acidic and alkaline H_2O and D_2O solutions.[21−23,26,28] On the other hand, the positive value of g for the Temkin adsorption isotherm shown in dashed line b of Figure 7 implies a lateral repulsive interaction between the adsorbed OPD H species, which leads to a decrease in $|\Delta G_\theta^0|$ of OPD H with θ ($0.2 < \theta < 0.8$).[40] As shown in dashed line b of Figure 7, the region $0.2 < \theta < 0.8$ corresponds to the short potential range (ca. 33 mV), which is difficult to observe in the Temkin adsorption isotherm correlating with the Frumkin adsorption isotherm. It is understood that the observation of the lateral repulsive interaction between the adsorbed OPD H species is difficult using other conventional methods. At other values of θ (i.e., $0 \le \theta < 0.2$ and $0.8 < \theta \le 1$), only the Frumkin adsorption isotherm is applicable to the adsorption of OPD H. Consequently, one can conclude that the Frumkin adsorption isotherm is more accurate, useful, and effective than the Temkin adsorption isotherm. The lateral attractive ($g < 0$) or repulsive ($g > 0$) interaction between the adsorbed OPD H species appears at $0.2 < \theta < 0.8$. The duality of the lateral attractive and repulsive interactions is a unique feature of the adsorbed OPD H species on the Pt, Ir, and Pt−Ir alloys in acidic and alkaline H_2O and D_2O solutions.

Standard Gibbs Energy of Adsorption. The standard Gibbs energy of adsorption of OPD H is given by the difference between the standard molar Gibbs energy of OPD H and that of a number of H_2O molecules on the adsorption sites of the Pt−Ir alloy surface in 0.5 M H_2SO_4 aqueous solution.[40,45] Under the Frumkin adsorption conditions, the relationship between the equilibrium constant (K) for OPD H and the standard Gibbs energy of adsorption (ΔG_θ^0) of OPD H is[40]

$$2.3RT \log K = -\Delta G_\theta^0 \qquad (8)$$

For the Pt−Ir alloy in 0.5 M H_2SO_4 aqueous solution, use of eqs 6 and 8 shows that ΔG_θ^0 of OPD H is in the range ($25.6 \ge \Delta G_\theta^0 \ge 19.4$) kJ·mol^{-1} for $K = 3.3 \cdot 10^{-5} \exp(2.5\theta)$ mol^{-1} and $0 \le \theta \le 1$. As stated above, this result implies an increase of $|\Delta G_\theta^0|$ of OPD H with θ ($0 \le \theta \le 1$).[40] It should be noted that ΔG_θ^0 is a negative number, that is, $\Delta G_\theta^0 < 0$. The standard Gibbs energies of adsorption (ΔG_θ^0) of OPD H and the equilibrium constants (K) for the Frumkin and Temkin adsorption isotherms of OPD H on the Pt, Ir, and Pt−Ir alloys in 0.5 M H_2SO_4 and 0.1 M KOH aqueous solutions are summarized in Tables 2 and 3, respectively.

Conclusions

On the Pt−Ir [90:10 % (by weight)] alloy in 0.5 M H_2SO_4 aqueous solution, the Frumkin and Temkin adsorption isotherms (θ vs E), the equilibrium constants [$K = 3.3 \cdot 10^{-5} \exp(2.5\theta)$ mol^{-1} for the Frumkin and $K = 3.3 \cdot 10^{-4} \exp(-2.1\theta)$ mol^{-1} for the Temkin adsorption isotherm], the interaction parameters ($g = -2.5$ for the Frumkin and $g = 2.1$ for the Temkin adsorption isotherm), the standard Gibbs energies of adsorption of OPD H [($25.6 \ge \Delta G_\theta^0 \ge 19.4$) kJ·mol^{-1} for $K = 3.3 \cdot 10^{-5} \exp(2.5\theta)$ mol^{-1} and $0 \le \theta \le 1$ and ($20.9 < \Delta G_\theta^0 < 24.0$) kJ·mol^{-1} for $K = 3.3 \cdot 10^{-4} \exp(-2.1\theta)$ mol^{-1} and $0.2 < \theta < 0.8$], and the rates of change of ΔG_θ^0 of OPD H with θ ($r = -6.2$ kJ·mol^{-1} for $g = -2.5$ and $r = 5.2$ kJ·mol^{-1} for $g = 2.1$) have been determined and are compared using the phase-shift method and correlation constants. The Frumkin adsorption isotherm is more accurate, useful, and effective than the Temkin adsorption isotherm. On the Pt, Ir, and Pt−Ir alloys in 0.5 M H_2SO_4 aqueous solution, the values of K for the Frumkin adsorption isotherms of OPD H decrease with increasing mass ratio of Ir. Negative values of g for the Frumkin adsorption isotherms of OPD H on the Pt, Ir, and Pt−Ir alloys in acidic and alkaline H_2O and D_2O solutions are experimentally and consistently determined.

For $0.2 < \theta < 0.8$, a lateral attractive ($g < 0$) or repulsive ($g > 0$) interaction between the adsorbed OPD H species appears. The duality of the lateral attractive and repulsive interactions is a unique feature of the adsorbed OPD H species on the Pt, Ir, and Pt−Ir alloys in acidic and alkaline H_2O and D_2O solutions.

The phase-shift method and correlation constants are the most accurate, useful, and effective way to determine the Frumkin, Langmuir, and Temkin adsorption isotherms of OPD H and related electrode kinetic and thermodynamic parameters of noble and highly corrosion-resistant metals (alloys) in acidic and alkaline H_2O and D_2O solutions.

Table 3. Comparison of the Standard Gibbs Energies of Adsorption (ΔG_θ^0) of OPD H and the Equilibrium Constants (K) for the Temkin Adsorption Isotherms (θ vs E) of OPD H on the Pt, Ir, and Pt−Ir Alloys in 0.5 M H_2SO_4 and 0.1 M KOH Aqueous Solutions

	ΔG_θ^0	K	
metal (alloy)/solution	kJ·mol^{-1}	mol^{-1}	ref
Pt−Ir alloy[a]/0.5 M H_2SO_4	$20.9 < \Delta G_\theta^0 < 24.0$	$3.3 \cdot 10^{-4} \exp(-2.1\theta)$	this work
Pt−Ir alloy[b]/0.5 M H_2SO_4	$21.1 < \Delta G_\theta^0 < 24.2$	$3.1 \cdot 10^{-4} \exp(-2.1\theta)$	21
Pt[c]/0.5 M H_2SO_4	$20.8 < \Delta G_\theta^0 < 24.1$	$3.5 \cdot 10^{-4} \exp(-2.2\theta)$	22
Ir[d]/0.5 M H_2SO_4	$21.5 < \Delta G_\theta^0 < 24.7$	$2.7 \cdot 10^{-4} \exp(-2.2\theta)$	22
Pt[e]/0.1 M KOH	$17.8 < \Delta G_\theta^0 < 21.0$	$1.2 \cdot 10^{-3} \exp(-2.2\theta)$	26
Ir[f]/0.1 M KOH	$18.3 < \Delta G_\theta^0 < 21.7$	$9.4 \cdot 10^{-4} \exp(-2.2\theta)$	26

[a] Pt−Ir [90:10 % (by weight)] alloy. [b] Pt−Ir [70:30 % (by weight)] alloy. [c] Pt (purity: 99.9985 %). [d] Ir (purity: 99.8 %). [e] Pt (purity: 99.9985 %). [f] Ir (purity: 99.8 %). The Temkin adsorption isotherms (θ vs E) are valid and effective only for $0.2 < \theta < 0.8$.

Supporting Information Available:

Comparisons of the measured and calculated values of the phase shift ($-\varphi$) for the optimum intermediate frequency ($f_o = 25.12$ Hz) on the Pt−Ir alloy in 0.5 M H_2SO_4 aqueous solution are summarized in Supplementary Table 1. The experimental and fitted data for the Frumkin adsorption isotherms of OPD H on the Pt, Ir, and Pt−Ir alloys in 0.5 M H_2SO_4 and 0.1 M KOH aqueous solutions are shown in Supplementary Figures 1 and 2, respectively. This material is available free of charge via the Internet at http://pubs.acs.org/.

Literature Cited

(1) Gileadi, E.; Kirowa-Eisner, E.; Penciner, J. *Interfacial Electrochemistry*; Addison-Wesley: Reading, MA, 1975.
(2) Gileadi, E. *Electrode Kinetics*; VCH: New York, 1993.

(3) Bockris, JO'M.; Khan, S. U. M. *Surface Electrochemistry*; Plenum Press: New York, 1993.
(4) Conway, B. E.; Jerkiewicz, G., Eds. *Electrochemistry and Materials Science of Cathodic Hydrogen Absorption and Adsorption, PV 94-21*: The Electrochemical Society: Pennington, NJ, 1995.
(5) Jerkiewicz, G. Hydrogen sorption at/in electrodes. *Prog. Surf. Sci.* **1998**, *57*, 137–186.
(6) Bockris, JO'M.; Reddy, A. K. N.; Gamboa-Aldeco, M. *Modern Electrochemistry*, 2nd ed.; Kluwer Academic/Plenum Press: New York, 2000; Vol. 2A.
(7) Jerkiewicz, G.; Feliu, J. M.; Popov, B. N., Eds. *Hydrogen at Surface and Interfaces, PV 2000-16*; The Electrochemical Society: Pennington, NJ, 2000.
(8) Gileadi, E., Ed. *Electrosorption*; Plenum Press: New York, 1967.
(9) Chun, J. H.; Ra, K. H. The phase-shift method for the Frumkin adsorption isotherms at the Pd/H_2SO_4 and KOH solution interfaces. *J. Electrochem. Soc.* **1998**, *145*, 3794–3798.
(10) Chun, J. H.; Ra, K. H. In *Hydrogen at Surface and Interfaces, PV 2000-16*; Jerkiewicz, G.; Feliu, J. M.; Popov, B. N., Eds.; The Electrochemical Society: Pennington, NJ, 2000 pp 159−173.
(11) Chun, J. H.; Ra, K. H.; Kim, N. Y. The Langmuir adsorption isotherms of electroadsorbed hydrogens for the cathodic hydrogen evolution reactions at the $Pt(100)/H_2SO_4$ and LiOH aqueous electrolyte interfaces. *Int. J. Hydrogen Energy* **2001**, *26*, 941–948.
(12) Chun, J. H.; Ra, K. H.; Kim, N. Y. Qualitative analysis of the Frumkin adsorption isotherm of the over-potentially deposited hydrogen at the poly-Ni/KOH aqueous electrolyte interface using the phase-shift method. *J. Electrochem. Soc.* **2002**, *149*, E325−330.
(13) Chun, J. H.; Ra, K. H.; Kim, N. Y. Langmuir adsorption isotherms of over-potentially deposited hydrogen at poly-Au and Rh/H_2SO_4 aqueous electrolyte interfaces: Qualitative analysis using the phase-shift method. *J. Electrochem. Soc.* **2003**, *150*, E207−217.
(14) Chun, J. H.; Jeon, S. K. Determination of the equilibrium constant and standard free energy of the over-potentially deposited hydrogen for the cathodic H_2 evolution reaction at the Pt-Rh alloy electrode interface using the phase-shift method. *Int. J. Hydrogen Energy* **2003**, *28*, 1333–1343.
(15) Chun, J. H. Methods for estimating adsorption isotherms in electrochemical systems. U.S. Patent 6,613,218, 2003.
(16) Chun, J. H.; Jeon, S. K.; Kim, B. K.; Chun, J. Y. Determination of the Langmuir adsorption isotherms of under- and over-potentially deposited hydrogen for the cathodic H_2 evolution reaction at poly-Ir/aqueous electrolyte interfaces using the phase-shift method. *Int. J. Hydrogen Energy* **2005**, *30*, 247–259.
(17) Chun, J. H.; Jeon, S. K.; Ra, K. H.; Chun, J. Y. The phase-shift method for determining Langmuir adsorption isotherms of over-potentially deposited hydrogen for the cathodic H_2 evolution reaction at poly-Re/aqueous electrolyte interfaces. *Int. J. Hydrogen Energy* **2005**, *30*, 485–499.
(18) Chun, J. H.; Jeon, S. K.; Kim, N. Y.; Chun, J. Y. The phase-shift method for determining Langmuir and Temkin adsorption isotherms of over-potentially deposited hydrogen for the cathodic H_2 evolution reaction at the poly-Pt/H_2SO_4 aqueous electrolyte interface. *Int. J. Hydrogen Energy* **2005**, *30*, 1423–1436.
(19) Chun, J. H.; Kim, N. Y. The phase-shift method for determining adsorption isotherms of hydrogen in electrochemical systems. *Int. J. Hydrogen Energy* **2006**, *31*, 277–283.
(20) Chun, J. H.; Jeon, S. K.; Chun, J. Y. The phase-shift method and correlation constants for determining adsorption isotherms of hydrogen at a palladium electrode interface. *Int. J. Hydrogen Energy* **2007**, *32*, 1982–1990.
(21) Chun, J. H.; Kim, N. Y.; Chun, J. Y. Determination of adsorption isotherms of hydrogen and hydroxide at Pt-Ir alloy electrode interfaces using the phase-shift method and correlation constants. *Int. J. Hydrogen Energy* **2008**, *33*, 762–774.
(22) Chun, J. Y.; Chun, J. H. Correction and supplement to the determination of the optimum intermediate frequency for the phase-shift method [Chun et al., *Int. J. Hydrogen Energy* **2005**, 30, 247−259, 1423−1436]. *Int. J. Hydrogen Energy* **2008**, *33*, 4962–4965.
(23) Chun, J. Y.; Chun, J. H. A negative value of the interaction parameter for over-potentially deposited hydrogen at Pt, Ir, and Pt-Ir alloy electrode interfaces. *Electrochem. Commun.* **2009**, *11*, 744–747.
(24) Chun, J. Y.; Chun, J. H. Determination of adsorption isotherms of hydrogen on titanium in sulfuric acid solution using the phase-shift method and correlation constants. *J. Chem. Eng. Data* **2009**, *54*, 1236–1243.
(25) Chun, J. H.; Chun, J. Y. Determination of adsorption isotherms of hydrogen on zirconium in sulfuric acid solution using the phase-shift method and correlation constants. *J. Korean Electrochem. Soc.* **2009**, *12*, 26–33.
(26) Chun, J.; Lee, J.; Chun, J. H. Determination of adsorption isotherms of overpotentially deposited hydrogen on platinum and iridium in KOH aqueous solution using the phase-shift method and correlation constants. *J. Chem. Eng. Data* **2010**, *55*, 2363–2372.
(27) Chun, J.; Kim, N. Y.; Chun, J. H. Determination of adsorption isotherms of hydroxide and deuteroxide on Pt-Ir alloy in LiOH solutions using the phase-shift method and correlation constants. *J. Chem. Eng. Data* **2010**, *55*, 3825–3833.
(28) Chun, J.; Kim, N. Y.; Chun, J. H. Determination of the adsorption isotherms of hydrogen and deuterium isotopes on a Pt−Ir alloy in LiOH solutions using the phase-shift method and correlation constants. *J. Chem. Eng. Data* **2010**, *55* (12), 5598–5607.
(29) Kvastek, K.; Horvat-Radosevic, V. Comment on "Langmuir adsorption isotherms of over-potentially deposited hydrogen at poly-Au and Rh/H_2SO_4 aqueous electrolyte interfaces; Qualitative analysis using the phase-shift method, *J. Electrochem. Soc.* **2003**, *150*, E207−217". *J. Electrochem. Soc.* **2004**, *151*, L9–10.
(30) Lasia, A. Comment on "The phase-shift method for determining Langmuir adsorption isotherms of over-potentially deposited hydrogen for the cathodic H_2 evolution reaction at poly-Re/aqueous electrolyte interfaces, *Int. J. Hydrogen Energy* **2005**, *30*, 485−499". *Int. J. Hydrogen Energy* **2005**, *30*, 913–917.
(31) Horvat-Radosevic, V.; Kvastek, K. Pitfalls of the phase-shift method for determining adsorption isotherms. *Electrochem. Commun.* **2009**, *11*, 1460–1463.
(32) Chun, J. H.; Ra, K. H.; Kim, N. Y. Response to comment on "Langmuir adsorption isotherms of over-potentially deposited hydrogen at poly-Au and Rh/H_2SO_4 aqueous electrolyte interfaces; Qualitative analysis using the phase-shift method, *J. Electrochem. Soc.* **2003**, *150*, E207−217". *J. Electrochem. Soc.* **2004**, *151*, L11–13.
(33) Chun, J. H.; Jeon, S. K.; Kim, N. Y.; Chun, J. Y. Response to comments on "The phase-shift method for determining Langmuir adsorption isotherms of over-potentially deposited hydrogen for the cathodic H_2 evolution reaction at poly-Re/aqueous electrolyte interfaces, *Int. J. Hydrogen Energy* **2005**, *30*, 485−499". *Int. J. Hydrogen Energy* **2005**, *30*, 919–928.
(34) In our e-mail communications, Horvat-Radosevic and Kvastek admitted that all their objections to the phase-shift method in ref 31 were confused and misunderstood. The exact same confusion and misunderstanding about the phase-shift method also appear in refs 29 and 30. They still do not understand and accept the phase-shift method itself without reliable simulation or experimental data.
(35) Gileadi, E.; Kirowa-Eisner, E.; Penciner, J. *Interfacial Electrochemistry*; Addison-Wesley: Reading, MA, 1975; pp 6, 72−73.
(36) Gileadi, E.; Kirowa-Eisner, E.; Penciner, J. *Interfacial Electrochemistry*; Addison-Wesley: Reading, MA, 1975; pp 86−93.
(37) Gileadi, E. *Electrode Kinetics*; VCH: New York, 1993; pp 291−303.
(38) Harrington, D. A.; Conway, B. E. AC impedance of faradaic reactions involving electrosorbed intermediates-I. Kinetic theory. *Electrochim. Acta* **1987**, *32*, 1703–1712.
(39) Gileadi, E.; Kirowa-Eisner, E.; Penciner, J. *Interfacial Electrochemistry*; Addison-Wesley: Reading, MA, 1975; pp 82−86.
(40) Gileadi, E. *Electrode Kinetics*; VCH: New York, 1993; pp 261−280.
(41) Bockris, J.O'M.; Khan, S. U. M. *Surface Electrochemistry*; Plenum Press: New York, 1993; pp 280−283.
(42) Bockris, J.O'M.; Reddy, A. K. N.; Gamboa-Aldeco, M. *Modern Electrochemistry*, 2nd ed.; Kluwer Academic/Plenum Press: New York, 2000; Vol. 2A, pp 1193−1197.
(43) Oxtoby, D. W.; Gillis, H. P.; Nachtrieb, N. H. *Principles of Modern Chemistry*, 5th ed.; Thomson Learning Inc.: New York, 2002; p 446.
(44) Gileadi, E. *Electrode Kinetics*; VCH: New York, 1993; pp 303−305.
(45) Gileadi, E. *In Electrosorption: Adsorption in Electrochemistry*; Gileadi, E., Ed.; Plenum Press: New York, 1967; pp 1−18.

Received for review August 14, 2010. Accepted December 25, 2010. This work was supported by the Research Grant of Kwangwoon University in 2010.

JE100837Q